New insights into extracellular matrix assembly and reorganization from dynamic imaging of extracellular matrix proteins in living osteoblasts

Pitchumani Sivakumar[1], Andras Czirok[2], Brenda J. Rongish[2], Vivek P. Divakara[1,3], Yu-Ping Wang[3] and Sarah L. Dallas[1,*]

[1]Department of Oral Biology, UMKC School of Dentistry, 650 E 25th Street, Kansas City, MO 64108, USA
[2]Department of Anatomy and Cell Biology, The University of Kansas Medical Center, 3901 Rainbow Boulevard, Kansas City, KS 66160, USA
[3]School of Computing and Engineering, UMKC, 5100 Rockhill Road, Kansas City, MO 64110, USA
*Author for correspondence (e-mail: dallass@umkc.edu)

Accepted 7 December 2005
Journal of Cell Science 119, 1350-1360 Published by The Company of Biologists 2006
doi:10.1242/jcs.02830

Summary

The extracellular matrix (ECM) has been traditionally viewed as a static scaffold that supports cells and tissues. However, recent dynamic imaging studies suggest that ECM components are highly elastic and undergo continual movement and deformation. Latent transforming growth factor beta (TGFβ) binding protein-1 (LTBP1) is an ECM glycoprotein that binds latent TGFβ and regulates its availability and activity. LTBP1 initially co-distributes with fibronectin in the extracellular matrix of osteoblasts, and depends on fibronectin for its assembly. To gain further insights into the mechanisms of assembly of LTBP1 and its spatial and temporal interactions with fibronectin, we have performed dual fluorescence time-lapse imaging of these two proteins in living osteoblasts using fluorescent probes. Time-lapse movies showed surprisingly large fibril displacements associated with cellular movement as well as occasional breaking of LTBP1 or fibronectin-containing fibrils. Individual fibrils stretched to as much as 3.5 times or contracted to as much as one fourth of their original length. Motile cells appeared to actively mediate extracellular matrix assembly by adding 'globules' or 'packets' of matrix material onto existing fibrils. They also actively reorganized the extracellular matrix by shunting matrix material from one location to another and exchanging fibrillar material between fibrils. This cell-mediated matrix reorganization was primarily associated with the assembly and remodeling of the initial (early) matrix, whereas mature, established ECM was more stable. Displacement vector mapping showed that different matrix fibrillar networks within the same cultures can show different dynamic motion in response to cell movement and showed that the motion of fibrils was correlated with cell motion. These data suggest novel cell-mediated mechanisms for assembly and reorganization of the extracellular matrix and highlight a role for cell motility in the assembly process.

Supplementary material available online at
http://jcs.biologists.org/cgi/content/full/119/7/1350/DC1

Key words: Dynamic imaging, Extracellular matrix, Fibronectin, LTBP1, Osteoblasts

Introduction

The extracellular matrix (ECM) controls cell function by regulating cell-matrix interactions, modulating extracellular signals and providing a storage site for growth factors and cytokines. The fibrillar and microfibrillar components of the ECM interact with each other and preserve tissue strength, elasticity and cohesiveness. However, the mechanisms by which the fibrillar proteins of the ECM are deposited and reorganized are still largely unknown.

Although type I collagen is the major component, the mineralized ECM of bone is also composed of several non-collagenous proteins with distinct functions (reviewed by Young, 2003). Fibronectin is one of the earliest proteins to be laid down in the ECM and is critical for cell adhesion, migration, angiogenesis and wound healing. The distribution of fibronectin in areas of skeletogenesis suggests that it may be involved in the early stages of bone formation (Gronowicz et al., 1991; Nordahl et al., 1995). In support of this, fibronectin has been shown to play a critical role in osteoblast differentiation and survival (Globus et al., 1998; Moursi et al., 1996). Several studies have suggested that fibronectin is required for assembly of multiple ECM proteins, including collagen types I and III (McDonald et al., 1982; Velling et al., 2002), fibulin (Godyna et al., 1995; Roman and McDonald, 1993), fibrinogen (Pereira et al., 2002) and thrombospondin (Sottile and Hocking, 2002). We have also previously shown that fibronectin is essential for assembly of latent TGFβ binding protein-1 (LTBP1) into the ECM of bone cells (Dallas et al., 2005).

LTBP1 is an ECM glycoprotein that binds and regulates TGFβ and is a member of the fibrillin superfamily. This family includes the fibrillins 1-3 (Corson et al., 2004; Kielty et al., 2002; Ramirez and Pereira, 1999), and LTBPs 1-4 (Hyytiainen et al., 2004). LTBP1 localizes to fibrillar structures in the ECM of bone and other tissues (Dallas et al., 1995; Taipale et al., 1996) and is thought to be critical for targeting TGFβ to the ECM as well as regulating TGFβ secretion and activation (Annes et al., 2004; Dallas et al., 1995; Flaumenhaft et al.,

1993; Miyazono et al., 1991; Taipale et al., 1994). We have previously shown that LTBP1 colocalizes with fibronectin in primary osteoblasts in a time-dependent manner (Dallas et al., 2002; Dallas et al., 2005). We have also shown that LTBP1 assembly is severely impaired in fibronectin-null embryonic fibroblasts and can be rescued by addition of exogenous fibronectin, suggesting that interactions between fibronectin and LTBP1 are critical for LTBP1 incorporation into the ECM (Dallas et al., 2005). TGFβ has been implicated in several bone diseases including bone metastatic cancer (reviewed by Guise and Chirgwin, 2003), osteoarthritis (Pujol, 1999), osteoporosis (Langdahl et al., 2003) and Camurati Engelman disease (Janssens et al., 2000; Kinoshita et al., 2000). Given the critical role of LTBPs in modulating TGFβ activity, it is important to understand the mechanism of assembly of LTBP1 in bone and its interactions with other matrix molecules.

Dynamic imaging and live-cell studies have been successfully used to monitor morphogenetic processes during embryonic development (Czirok et al., 2004; Czirok et al., 2002; Jones et al., 2005; Sakai, 2003) and to gain quantitative insights into various cellular processes (Eils and Athale, 2003). The use of recombinant fluorescent protein technology and pH-sensitive dyes to tag virtually any cellular structure and the advent of powerful imaging techniques such as FRET and confocal microscopy, have enabled researchers to obtain biochemical, biophysical, spatio-temporal and kinetic information on cells and cellular components (reviewed by Day and Schaufele, 2005; Parsons et al., 2004; Sekar and Periasamy, 2003). These dynamic imaging approaches have recently been used to monitor the kinetics of assembly of ECM proteins in cell cultures (Ohashi et al., 1999; Petroll et al., 2004; Petroll and Ma, 2003; Petroll et al., 2003; Kozel et al., 2006; Czirok et al., 2006) and developing embryos (Czirok et al., 2004; Davidson et al., 2004; Filla et al., 2004). These studies suggest that ECM components are highly elastic and undergo continual movements and deformations in response to cell movement and morphogenesis. To obtain further insights into the interactions between fibronectin and LTBP1 and to examine their co-assembly into the ECM, we have performed dynamic time-lapse imaging studies in living osteoblast cultures with fluorescently labeled fibronectin and LTBP1 probes. Our findings suggest that these proteins undergo surprisingly large deformations in response to cell movement and that their fibril dynamics are different in early versus mature ECM. We provide new evidence for active participation of the cells in fibril assembly, and evidence that cells can reorganize the ECM by shunting fibrillar material from one location to another. In addition, we have used computational analyses to quantify the ECM fibril dynamics and show that cell and fibril motions are correlated.

Results

Incorporation and stability of fluorescently labeled fibronectin and LTBP1 probes

Time-course incubation studies using day 3 fetal rat calvarial osteoblast (FRC) cultures showed that the fibronectin probe incorporated rapidly by 1.5 hours of incubation, whereas incorporation of the LTBP1 probe was optimal after 4 hours (data not shown). By 24 hours, a well-defined fibrillar network was observed. The majority of the LTBP1 staining was colocalized with fibronectin. Fluorescent staining with both probes appeared stable up to approximately 8 days after removal of the probe (data not shown). However, by 10 days, the fibrillar staining was lost, presumably due to internalization of the probe and/or fluorescent tag. A 3 hour incubation with fluorescent probes was used for subsequent imaging studies.

Time-lapse movies show dynamic movements of cells and fibrils

Time-lapse imaging of fibronectin and LTBP1-positive fibrils in early (day 2) postconfluent FRC cultures revealed that these fibrillar networks were highly dynamic. A large amount of cellular movement was observed, resulting in continual stretching and contracting of the fibrils. Fig. 1 shows a still image frame of fibronectin fibrils at the start of time-lapse imaging in a 2 day FRC culture from Movie 1 in the supplementary material. Upon viewing this movie it is clear that the entire fibrillar network is constantly being stretched and contracted as a result of cell motion. The arrows marked A, B, C and D in Fig. 1 point to individual fibrils that show particularly dramatic dynamic movements as described in further detail in Figs 2 and 3, and Movies 2 and 3 in supplementary material.

Fig. 2 shows a time-lapse image series depicting a cropped view of fibrils A and B from Fig. 1. The corresponding cell images and merged cell and fibril images are also shown. Note that fibrils A and B appear joined at zero hours. These fibrils then gradually pull apart (2-10 hours) and are separated by 19 hours. On the merged images (6-12 hours), it can be seen that these fibrils are lying on cellular processes and that the retraction of these processes results in pulling apart of the fibrils. The cell and fibril dynamics shown in Fig. 2 can be more clearly seen by viewing Movie 2 in supplementary material. Note also, that the entire fibrillar network shows deformations and dynamic motion during the imaging period. To illustrate the motion of cells in the image field in Fig. 2, the nuclei of three individual cells have been outlined in blue, green or red and their motion paths (trajectories), over a time-frame of 19

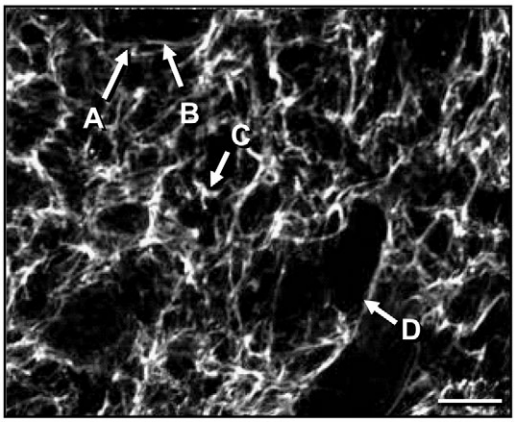

Fig. 1. Image field from a day 2 FRC culture at the start of dynamic imaging. This image corresponds to the bottom left panel of Movie 1 in supplementary material and represents Alexa Fluor 488-labeled fibronectin fibrils. Arrows labeled A-D indicate individual fibrils that show dramatic motions (see Figs 2 and 3 for description of individual fibril dynamics) Bar, 50 μm.

hours, have been plotted using the Image J software with the 'Manual tracking' plug-in. The trajectories for the entire 19-hour movie are shown in the bottom panel. The cell with the blue outlined nucleus moves towards the lower left of the image: a distance of 127 μm. The cell whose nucleus is outlined in green traverses down almost the entire field of view, a distance of 149 μm. The cell whose nucleus is outlined in red comes from outside the image field and moves towards the bottom left, traveling a distance of 87 μm. Movie 2 in supplementary material also shows the trajectories of these cells superimposed on the movie.

Time-lapse movies reveal potential mechanisms for cell-mediated assembly and reorganization of the ECM

A number of novel observations were made from the dynamic movies concerning potential mechanisms for cell-mediated assembly and reorganization of the ECM. Motile cells appeared to reorganize existing ECM fibrils by shunting 'globules' or 'packets' of ECM material from one location to another. Exchange of fibrillar material between fibrils was also observed, which appeared to be mediated by motile cells. Examples of these are shown in Fig. 3, which presents a time-lapse image series of an enlarged view of fibrils C and D from

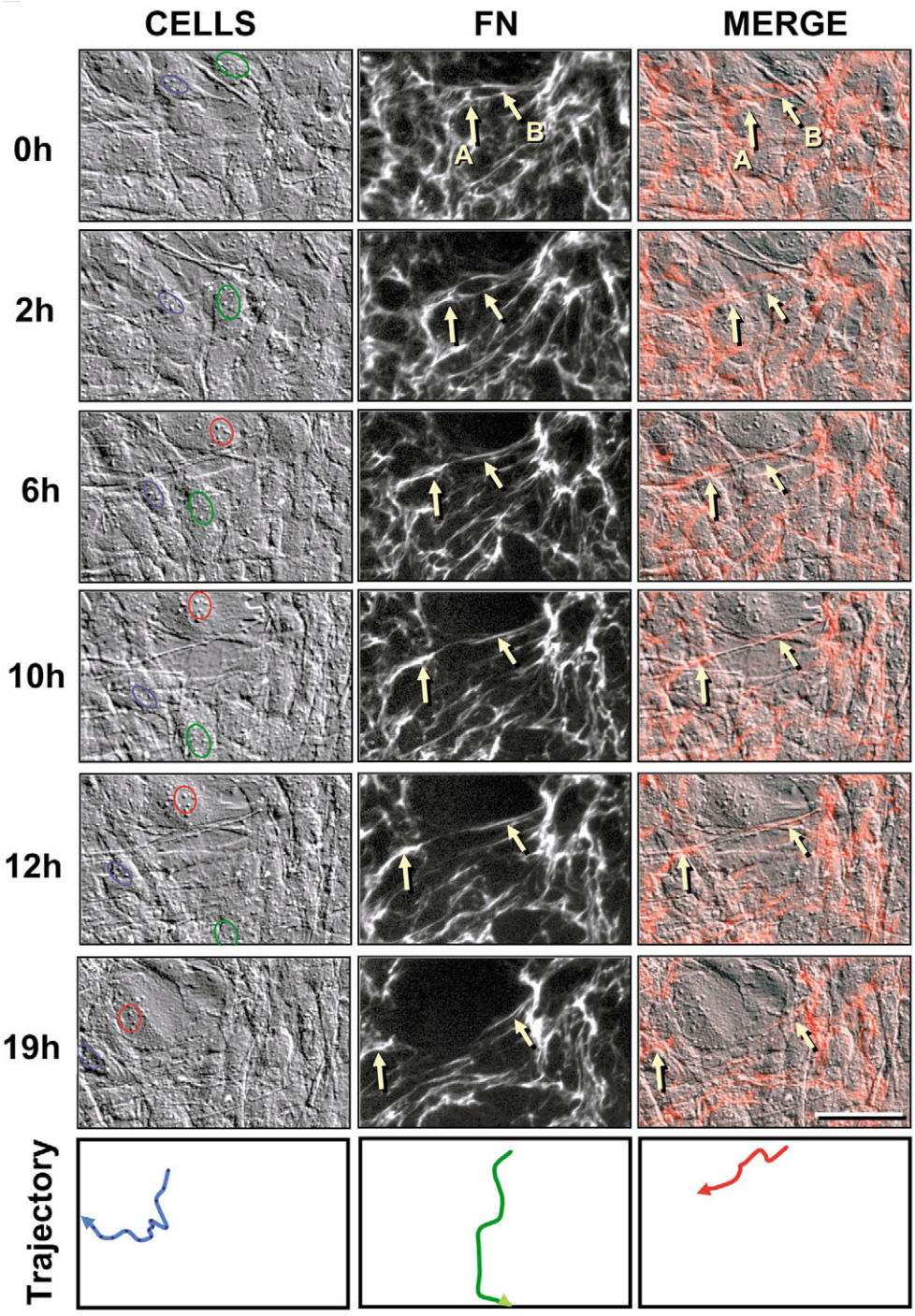

Fig. 2. Cell and fibronectin fibril dynamics in a day 2 FRC culture. Time-lapse image series showing the dynamic motion of fibrils A and B from Fig. 1. Corresponding images are shown for the cells (viewed by DIC) and fibronectin (FN) fibrils. Merged images in which the fibronectin fibrils are pseudocolored red are shown on the right. The blue, green and red circles are the outlines of nuclei on individual cells that show significant movement during the 19 hour period. The motion paths (trajectories) of these cells are indicated below the image series. Arrows in the fibronectin images indicate two fibrils (A and B) that appear joined at 0 hours, but gradually pull apart until they are separated by 16 hours. Corresponding arrows on the merged pictures indicate that these fibrils lie on cellular processes and become separated upon retraction of these processes. A movie corresponding to these still images is available as Movie 2 in supplementary material. Bar, 50 μm.

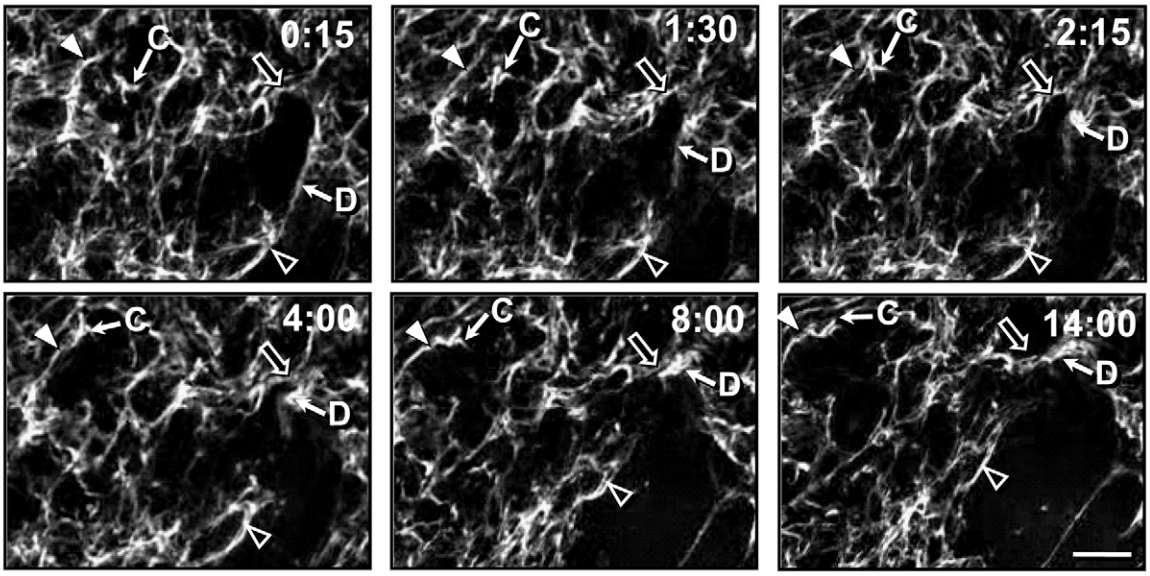

Fig. 3. Cell-mediated shunting and exchange of fibrillar material. Time-lapse image series showing examples of cell-mediated 'shunting' of fibrillar ECM material and 'exchange' of fibrillar material from one fibril to another. The image series shows an enlargement of fibrils C and D from Fig. 1. Fibril C moves upwards and to the left and by 4 hours, becomes joined with another fibril indicated by the white arrowhead. Fibril D appears joined at zero hours with a fibril indicated by the open arrowhead. By 1 hour 30 minutes, fibril D has detached from this fibril. It then retracts and moves upwards and to the left to become joined to a different fibril, indicated by the open arrow. See Movie 3 in supplementary material. Bar, 50 μm.

Fig. 1. Fibril C indicates a piece of fibronectin-positive material resembling an inverted Y. This fragment is shunted upwards and to the left. By 4 hours, the fragment becomes joined to another fibril (white arrowhead). The joined fibrils then appear to behave as a single fibril (i.e. their motion appears as a joined unit rather than as individual fibrils). Fibril D shows an example of fibril exchange. This fibril is initially joined to another fibril indicated by the open arrowhead. Fibril D then pulls away, contracts, moves upwards and to the left and appears to join with a different fibril, indicated by the open arrow. Note also that the entire fibrillar network shows distortions and deformations over the imaging period. These processes of fibril exchange and shunting can be more clearly seen in Movie 3 in supplementary material corresponding to Fig. 3. The movie also shows the movement of cells in the same field.

In the example shown in Fig. 4, a piece of fibrillar material (arrowhead) appears to be added to the end of a Y-shaped fibril (arrow). This can be more clearly seen in Movie 4 in supplementary material in which the movement of the ECM material and associated cell movement can be observed. From this movie, it appears that a cell moving in the same direction carries this piece of fibrillar material which is then added onto the end of the fibril. Such cell-mediated addition of fibrillar material to fibril ends may represent a mechanism for ECM fibril growth. Occasionally in these time-lapse movies, cells exerted forces strong enough to break individual fibronectin or LTBP1 fibrils (data not shown). The snapped ends of the fibril showed elastic recoil, suggesting that the fibrils may exist in a state of tension.

Dual imaging of LTBP1 and fibronectin fibrillar networks in early and mature FRC cultures

To compare the relative dynamics of LTBP1 and fibronectin fibrils, we next performed time-lapse microscopy with simultaneous labeling of both LTBP1 and fibronectin fibril

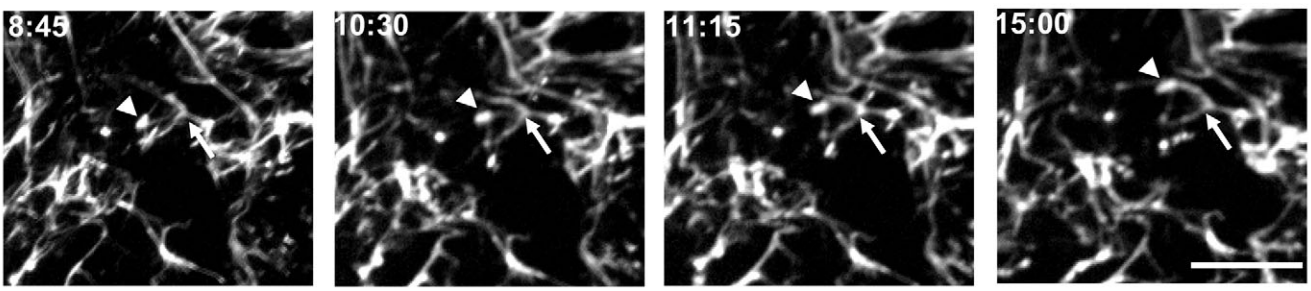

Fig. 4. Addition of a piece of ECM material to the end of a fibril. Time-lapse image series showing the addition of a small piece of ECM material (arrowhead) onto a Y-shaped fibril (arrow). Note that this piece of fibrillar material is gradually moved upward and added on to the end of the Y-shaped fibril (Bar=25 μm). A movie showing this addition event and the associated cell movement is available as Movie 4 in supplementary material.

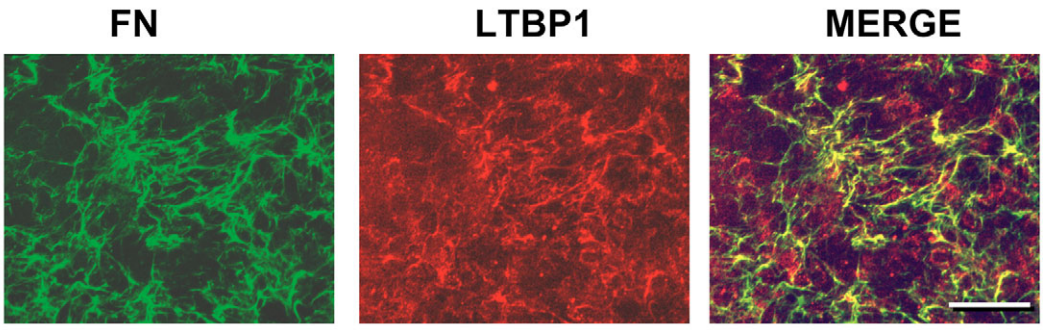

Fig. 5. Dual imaging of fibronectin and LTBP1 in a day-2 FRC culture. Still image frames taken at the start of time-lapse imaging in a day 2 FRC culture using fluorescent probes for fibronectin (FN, green) and LTBP1 (red). Note that the fibrillar staining for LTBP1 is predominantly colocalized with fibronectin, as indicated by the yellow areas in the merged image. However, the LTBP1 probe also gives some staining of the cells. A movie corresponding to these images is available as Movie 5 in supplementary material and shows that both fibrillar networks undergo continual stretching and contraction in response to cell movement. Bar, 100 μm.

networks. A comparison was made between early (day 2) and mature (day 12) FRC cultures.

In day 2 cultures, much of the staining for LTBP1 (red) was colocalized with fibronectin (green) in similar fibrillar networks as shown by the still images in Fig 5. In addition to fibrillar staining, the LTBP1 antibody probe also gave some staining of the cells. The yellow fluorescence in the merged image indicates colocalization of LTBP1 and fibronectin in fibrils that showed identical movements (see Movie 5, supplementary material). Again a large amount of dynamic movement was observed, resulting in continual stretching and contracting of the LTBP1/fibronectin-positive fibrils. Similar shunting, exchange and fibril addition events as described above were observed with both ECM proteins.

We have previously shown that although LTBP1 and fibronectin are initially colocalized in early FRC cultures, in mature (2-3 week) cultures, they are localized in distinct fibrillar networks, suggesting ECM reorganization and/or partitioning (Dallas et al., 2005). We therefore performed dynamic imaging studies to determine the dynamic properties of LTBP1 and fibronectin-positive fibrils in mature (12 day) FRC cultures with a highly organized ECM and to determine whether these different fibrillar networks showed similar or different fibril dynamics. Fig. 6A shows still images from a time-lapse movie from a day 12 FRC culture. In contrast to the day 2 cultures, LTBP1 and fibronectin were found in separate fibrillar networks in these mature FRC cultures. The LTBP1 (red) appeared as long fibrils, mainly in parallel arrays, that were distinct from the shorter, more randomly oriented fibronectin fibrils (green). Confocal microscopy indicated that the LTBP1 fibrils were localized in a layer above the fibronectin fibrils and that the fibronectin fibrils were closer to the cells (data not shown). Surprisingly, a large amount of cell movement was observed, even in 12-day postconfluent cultures, resulting in the continual stretching and contracting of the ECM fibrils. Interestingly, the displacements of the LTBP1-positive fibrils appeared to be less than those of fibronectin fibrils. A movie corresponding to this image field is presented as supplementary material Movie 6. Fig. 6B shows an enlarged view of the boxed area in Fig. 6A. Here a green fibronectin fibril (large arrow) stretches and contracts dramatically over the 18-hour imaging period. However, the overlying red LTBP1-positive fibrils (example indicated by small arrow) in the same region show much smaller displacements. The trajectories of these two fibrils, obtained by tracking the co-ordinates of one end of each fibril, are also presented in this figure. Note that the LTBP1 fibril has a much shorter trajectory compared with the fibronectin fibril. These differences in the dynamic movements of LTBP1 and fibronectin fibrils can be more clearly seen in supplementary material Movie 7.

Quantification of fibril dynamics shows that more matrix reorganization events occur in early ECM compared with mature ECM

To obtain an estimate of the frequency of occurrence of the different types of fibril dynamic events, six independent movies from day 2 FRC cultures and five independent movies from day 12 cultures were analyzed quantitatively. Based on our observations from the movies, we hypothesized that the mature ECM fibrils are more stable than those in the immature matrix and therefore would show a reduced number of fibril dynamic events (shunting, exchange, addition, breaking). To test this, a 4×3 grid was superimposed on the movies to facilitate counting and four categories of fibril dynamics were quantified: (1) Shunting events where discrete 'packets', 'globules' or fragments of ECM material were shunted from one location to another; (2) Addition events where small globules or packets of fibrillar material were added to ends of fibrils; (3) Exchange events where two fibrils joined and/or fibrillar material was translocated from one fibril to another; (4) Breaking events where there is an 'instantaneous' snapping of fibrils between successive image frames, followed by elastic recoil of the fibril ends. Table 1 shows the results from the quantitative analysis of fibril dynamic events. In both day 2 and day 12 cultures, fibril shunting events were the most common, occurring as many as 27 times per image field. Addition events were the next most frequent, followed by fibril exchange. Breaking events were rare, occurring only between 0.2 and 0.5 times per image field. Interestingly, all categories of fibril dynamic events, except fibril breaking, were significantly reduced in mature cultures compared with day 2. This was particularly striking in the case of the LTBP1 fibrils in 12-day cultures, in which there was a three- to tenfold reduction in shunting, addition and exchange events compared with day 2 cultures. In day 12 cultures, there were also significantly fewer dynamic events occurring in LTBP1-positive fibrils compared with fibronectin fibrils, suggesting that these different ECM fibrillar networks had different dynamic properties.

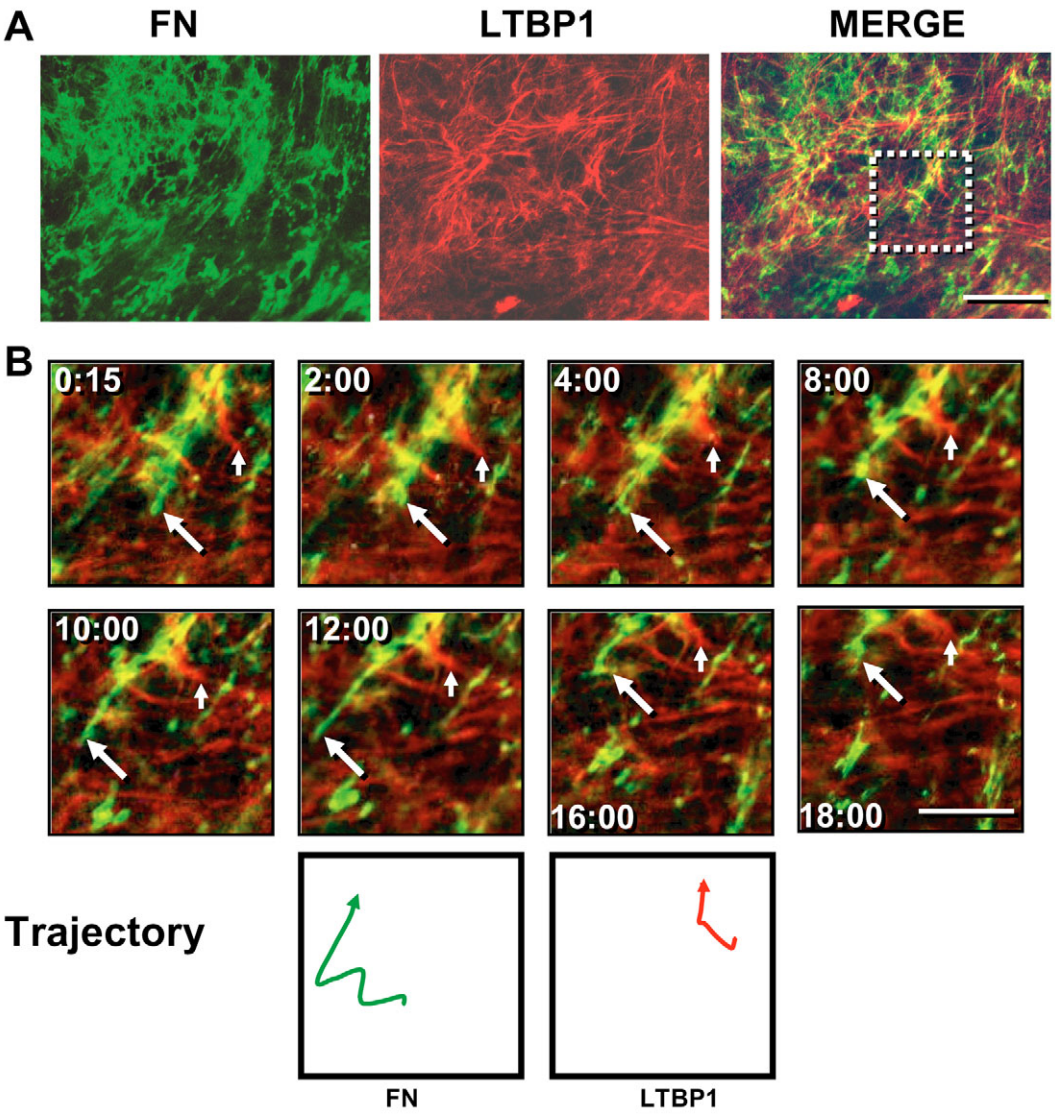

Fig. 6. Dual imaging of fibronectin and LTBP1 in a day-12 FRC culture. (A) Still image frames taken at the start of time-lapse imaging in a day 12 FRC culture using fluorescent probes for fibronectin (green) and LTBP1 (red). Note that the LTBP1 and fibronectin fibrils are localized in separate fibrillar networks. Movie 6 in supplementary material shows that both fibrillar networks undergo continual stretching and contraction in response to cell movement. (B) Time-lapse image series from the boxed area in A. Note a fibronectin fibril (large arrow) that stretches between 15 minutes and 4 hours, then contracts between 4 and 8 hours. The fibril then stretches again to reach its maximal length at 12 hours, then contracts again between 12 and 18 hours. Also note an LTBP1 fibril (small arrow) in the same region that appears to show much less motion compared with the fibronectin fibril. The bottom panel shows the trajectories of these fibrils obtained by tracking the co-ordinates of the end of each fibril in the image series and confirms that the LTBP1 fibril traverses a smaller trajectory. See also Movie 7 in supplementary material. Bar, 100 μm (A); 50 μm (B).

LTBP1-positive fibrils in mature (day 12) cultures show less stretching compared with LTBP1 fibrils in immature (day 2) cultures

Based on our observations from the movies we hypothesized that the ECM fibrils in mature (day 12) FRC cultures stretched and contracted much less than fibrils in the early (2 day) cultures, i.e. they were more rigid and less elastic. To test this, measurements were performed on 15 independent LTBP1 and fibronectin fibrils from day 2 and day 12 movies using the analySIS image processing software. Two fiducial points were identified on each fibril and the fibrillar distance between these markers was measured on sequential images. The maximal percent stretch and maximal percent contraction were determined for each fibril and the mean calculated. Table 2 shows that the mean maximal percent stretch and maximal percent contraction for LTBP1-positive fibrils was reduced approximately sixfold in day 12 FRC cultures compared with day 2 cultures, suggesting that the fibrils in the mature cultures were more rigid compared with the initially assembled fibrils. Interestingly, the mean maximal percentage stretch and contraction were not significantly different for fibronectin at day 12 compared with day 2, suggesting that the fibronectin fibrils retained their elastic properties in mature cultures. The maximal stretch recorded

Table 1. Comparison of LTBP1 and fibronectin fibril dynamics in early versus mature FRC cultures

	Mean ± s.e.m. per image field (0.14 mm^2)			
Event	FN (day 2) (n=6)	LTBP1 (day 2) (n=6)	FN (day 12) (n=5)	LTBP1 (day 12) (n=5)
Fibril shunting	27.3±1.2	21.7±0.9*	16.6±0.9*,†	6.0±0.3*,†,‡
Fibril addition	6.5±0.6	5.0±1.2*	4.2±0.4*	1.4±0.2*,†,‡
Fibril exchange	3.16±0.3	2.0±0.3*	2.2±0.4*	0.2±0.2*,†,‡
Fibril breaking	0.5±0.3	0.3±0.2	0.2±0.2	0±0

LTBP1 and fibronectin fibril dynamics were quantified in day 2 and day 12 FRC cultures by counting the number of fibril shunting, addition, exchange and breaking events within a 4×3 grid superimposed on the movies, according to the definitions provided in the text. *Significantly different from FN at day 2; †significantly different from LTBP1 at day 2; ‡significantly different from FN at day 12 (P<0.05, ANOVA, followed by Student Newman Keuls test).

for any single fibril was 251% and the maximal contraction was 73%.

Computational analysis shows that different fibrillar networks can have different dynamic properties

To gain further quantitative insights into the dynamic properties of these ECM molecules and to correlate cell and fibril motion we have developed computational methods to quantify the overall displacements of the cells and the fibrillar networks. First, displacement mapping analysis was performed (see Materials and Methods). In this technique, 100 point markers are positioned on recognizable features on an image frame from a movie. The same markers are then placed on an image taken 1 hour later, and repositioned if the feature has moved. The displacement of each point marker is determined and mean displacements calculated. Fig. 7A shows a frequency distribution plot of displacements of point markers positioned on cell, fibronectin or LTBP1 images from a day 2 FRC movie. Note that the majority of the displacements are between 0-6 μm/hour. As expected, owing to the predominant colocalization of LTBP1 and fibronectin at day 2, the displacements of point markers on these fibrillar networks were very similar. The mean displacements of point markers (mean ± s.e.m.) on cells (4.36±0.16 μm), fibronectin (3.91±0.19 μm) and LTBP1 fibrils (3.91±0.19 μm) were not significantly different. In day 12 cultures, owing to multilayering of the cells, it was not possible to reliably track point markers (usually nucleoli) on the cell images. Therefore, data were obtained only for the displacement of LTBP1 and fibronectin-positive fibrils. Interestingly, in day 12 cultures, when LTBP1 and fibronectin were localized in distinct fibrillar networks, there were significant differences in the movement of point markers on the LTBP1 compared with fibronectin fibrillar networks. As shown by the frequency distribution plot (Fig. 7B), there were more markers that moved a distance greater than 6 μm in the fibronectin images compared with LTBP1, whereas the number of markers that moved less than 3 μm was higher for LTBP1 than fibronectin. These differences were also reflected in the mean displacements. Thus, in day 12 cultures, the mean displacements of point markers (mean ± s.e.m.) for fibronectin and LTBP1 were 3.31±0.13 and 1.82±0.24, respectively (P<0.05), confirming that different fibrillar networks can have different dynamic properties.

Table 2. Comparison of LTBP1 and fibronectin fibril stretching and contraction in early versus mature FRC cultures

	Day 2		Day 12	
	FN	LTBP1	FN	LTBP1
Mean maximal percentage stretch	60.0±17.6 (n=12)	65.0±18.4 (n=12)	58.8±12.2 (n=14)	9.6±1.6*,† (n=15)
Mean maximal percentage contraction	37.0±5.0 (n=14)	36.5±6.0 (n=14)	28.3±6.0 (n=11)	10.5±1.3* (n=15)

The changes in lengths of 15 independent fibrils of fibronectin and LTBP1 in day 2 and day 12 cultures were measured using the analySIS image processing software. Two fiducial points were identified on each fibril and the fibrillar distance between these markers was measured on sequential time-lapse images. The maximal percentage stretch and maximal percentage contraction were determined for each fibril and the mean was calculated. (Note that individual n values in the table may vary as only those fibrils that showed stretching or showed contraction were included in the analysis, e.g. of the 15 fibrils measured for fibronectin at day 2, n=12 showed stretching and n=14 showed contraction.) *Significantly different from LTBP1 at day 2; †significantly different from FN at day 12 (Kruskal Wallis test, followed by Dunn's post-hoc test).

Correlation analysis of displacement vectors shows that the direction of movement of cells and fibrils are significantly correlated

To compare the direction of movement of the cells and fibrils, we performed a vector correlation analysis. Vector maps were

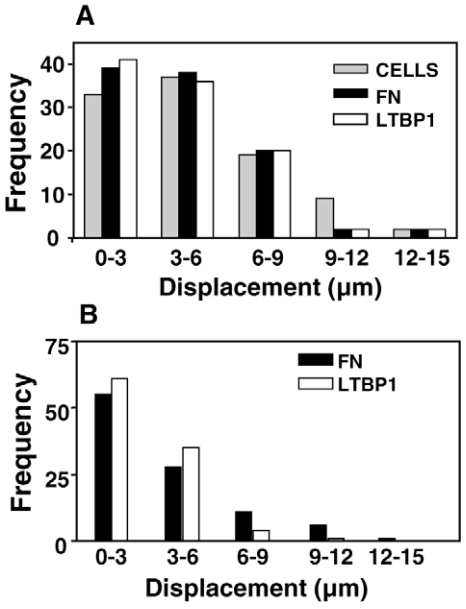

Fig. 7. Displacement mapping analysis of cell and fibril movement (see Materials and Methods for description of technique). Frequency distribution plots showing displacements of point markers positioned on cell, LTBP1 or fibronectin fibril images during a time interval of 1 hour in day 2 (A) and day 12 (B) FRC cultures. Note that the movement of cells, LTBP1 and fibronectin (FN) fibrils in day 2 cultures are very similar. However, in day 12 cultures, the number of markers that moved distances greater than 6 μm was higher for fibronectin compared with LTBP1. Mean displacements for fibronectin and LTBP1 markers were significantly different at day 12 but not day 2 (see text).

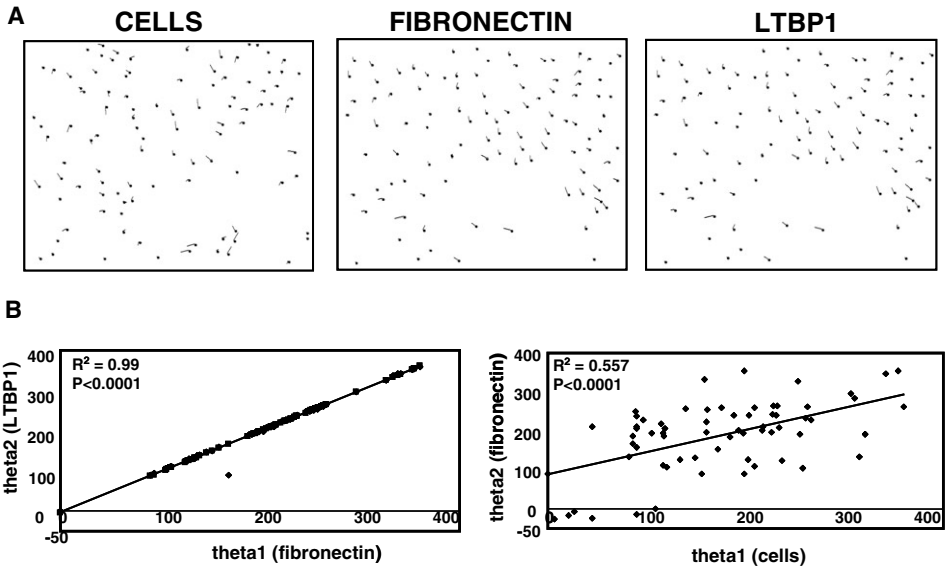

Fig. 8. Correlation of cell and fibril motion. (A) Vector maps depicting the direction of movement of point markers on cells and fibrils in day 2 FRC cell cultures. These vector maps were generated from still images from Movie 1 in supplementary material. 100 point markers were positioned on features in a still image of cells or fibrils. The same features were identified on an image obtained 1 hour later and the markers repositioned if they had moved. Vectors depicting the displacement of the point markers were generated in which the dots represent the initial position of each point marker, and the end of the line represents the position to which the point marker has moved. Note that the direction of movement of point markers on cell and fibril images appears generally correlated. (B) Graphs showing correlation of the direction of movement of vectors on cell and fibril images from day 2 cultures compared using the 'local average' analysis (see Materials and Methods section). This software calculates the average angle of vector movement within paired local neighborhoods within a 30 μm radius from comparison images of fibronectin/LTBP1 or cells/fibronectin. The pairs of angles from equivalent neighborhoods in each image were plotted and the correlation coefficient calculated. Note that there was a strong correlation between the movement of fibronectin and LTBP1 vectors, as expected because these two ECM molecules were colocalized. The movement of vectors on cell images was also significantly correlated with the movement of fibronectin vectors. Similar results were obtained comparing cell and LTBP1 vectors (data not shown).

generated using co-ordinates of the point markers used for displacement analysis. Fig. 8A shows examples of vector maps depicting movement of point markers on cell, LTBP1 and fibronectin images from a day 2 FRC culture. Note that the point markers on fibronectin and LTBP1-positive fibrils have identical directions of movement in the day 2 culture, consistent with their predominant colocalization. The movement of point markers on cells, although not identical, appears to follow the same general pattern.

To verify quantitatively whether the motion of cells and fibrils was correlated, we performed a 'local average correlation', in which the average angle of vectors within paired local neighborhoods a 30 μm radius were plotted for comparisons between cells-fibronectin, cells-LTBP1 and fibronectin-LTBP1 (see Materials and Methods for details of this analysis). Fig. 8B shows examples of local average correlations from a day 2 movie. As expected, the correlation between vector angles for LTBP1 and fibronectin fibrils was very close to 1, as these ECM proteins are predominantly colocalized at day 2 (R^2=0.99, P<0.0001) (see Fig. 8B). There was also a significant correlation between vector angles for comparisons between cell motion and fibronectin fibril motion (Fig. 8B) (R^2=0.557, P<0.0001). An identical correlation was obtained between cell motion and LTBP1 fibril motion (R^2=0.557, P<0.0001) (data not shown). Similar analyses were performed on four independent movies and in all cases, a significant correlation was obtained for comparisons of fibronectin and LTBP1 fibril movement and for cell movement compared with LTBP1 or fibronectin fibril movement (data not shown). As further confirmation of these data, a similar analysis was performed using pairs of 'nearest neighbor' vectors, which gave essentially identical results (data not shown).

We have also compared the difference in angles between pairs of average vectors from cell and fibril images (data not shown). As expected, the majority of the angle differences between pairs of vectors on cell images and LTBP1 images or cell images and fibronectin images were between 0-90° suggesting that they were moving in similar directions. Chi-square analysis was statistically significant (P<0.001), rejecting the null hypothesis that the angle differences are randomly distributed between 0-180°.

Discussion

In this study, we have described the dual epifluorescence imaging of two ECM proteins, fibronectin and LTBP1, in living osteoblast cultures and made a number of novel observations. (1) We have simultaneously imaged cells together with two different ECM proteins in living osteoblast cultures over extended time periods of up to 24 hours and demonstrated extensive ECM fibril motion in both immature and mature cultures; (2) we have presented data suggesting a novel mechanism for the initial assembly and reorganization of ECM fibrils by cells actively shunting ECM material from one location to another and exchanging material between fibrils; (3) we have quantitatively compared ECM fibril dynamics in early (day 2) osteoblast cultures and mature (day 12) cultures and shown that the ECM in mature cultures is more stable than in immature cultures and is less subject to cell-mediated reorganization; (4) we have quantitatively analyzed cell and fibril motions and shown that they are correlated; (5) we have quantitatively demonstrated for the first time that different fibrillar networks within the same culture can show different dynamic properties.

The present studies confirm and extend the findings of Ohashi and co-workers, who investigated the dynamics of early fibronectin assembly using GFP-tagged fibronectin expressed in subconfluent CHO cells, that elaborate a less extensive

matrix than the FRC cells (Ohashi et al., 1999; Ohashi et al., 2002). Their studies, performed over a 0-4.5 hour imaging period, showed that the fibronectin fibrils were highly 'elastic' and that cells could exert forces sufficient to break individual fibronectin fibrils. In the present study, we have extended these studies to compare fibronectin and LTBP1 fibril dynamics in early FRC cultures that have a newly assembled ECM as well as in mature cultures with a well established ECM.

One of the most important findings of the present study is the observation that motile cells may actively participate in the assembly and reorganization of ECM proteins. This is evidenced by movies in which cells appear to move 'packets' or 'globules' of ECM material and deposit them onto the ends of fibrils as well as examples of cell-mediated 'shunting' of ECM material from one location to another and/or exchange of material between fibrils. A recent study has shown a similar assembly mechanism for elastin, in which cell-surface-associated globules of elastin were deposited onto pre-existing elastic fibers that coalesced into larger structures (Kozel et al., 2006). Such cell-mediated movement of ECM material could represent a novel mechanism for ECM assembly and may provide a mechanism for reorganization/ remodeling of the ECM without the requirement of proteolytic action. Interestingly, Sottile and co-workers have recently shown, using fibronectin-null cells, that the withdrawal of fibronectin from these cultures results in loss of matrix fibrils of fibronectin, collagen and thrombospondin. This loss of ECM appears to occur independent of protease activity, supporting the notion that the ECM can be remodeled by protease-independent mechanism(s) (Sottile and Hocking, 2002).

Another highly significant finding is our quantitative observation that the ECM in mature cultures appeared to be more stable than in immature cultures, particularly in the case of the LTBP1-positive fibrils. This is supported by displacement mapping, showing that the mean displacements of LTBP1 and fibronectin fibrils are reduced in mature cultures, as well as quantitation of dynamic events, showing that there is a reduction in cell-mediated ECM reorganization events. Measurements of fibril stretching indicated that the LTBP1-positive fibrils in mature cultures also showed a limited or no capacity to stretch, compared with those in immature cultures. However, the fibronectin fibrils appeared to retain their elastic properties. Together, these data suggest that cell-mediated matrix reorganization events may be primarily associated with initial ECM assembly, but that the mature ECM is more stable, potentially due to crosslinking of ECM macromolecules and/or a higher level of ECM organization. An alternative explanation is that as more ECM is deposited and the ECM macromolecules become further away from the cells, they become less influenced by cell motion and therefore less subject to cell-mediated reorganization events.

At present, the significance of ECM fibril dynamics in vivo is unclear as few studies have addressed this in vivo. However, it does seem highly likely that ECM fibril dynamics are significant in the whole animal, particularly during the process of morphogenesis in embryonic development. A recent study by Czirok et al. (Czirok et al., 2004) described extensive large-scale repositioning of fibrillin-2-containing fibrils in developing avian embryos. Dynamic remodeling of fibronectin fibrils has also been shown to occur during gastrulation and neurulation in developing frog embryos (Davidson et al., 2004). As a large amount of cell motion and ECM assembly occurs during fracture healing, it also seems likely that ECM fibril dynamics may be a crucial component of the fracture repair process in bone. We have recently performed live-cell imaging studies on isolated neonatal calvarial explants and observed that the cells of bone, including both osteoblasts and osteocytes do show a large amount of dynamic motion, consistent with the current observations using primary osteoblast cultures (S.L.D., unpublished observations).

By immunostaining, we have previously shown that LTBP1 and fibronectin are colocalized in the ECM of early FRC cultures but are localized in separate fibrillar networks in mature cultures, suggesting that matrix partitioning or reorganization occurs as a function of ECM maturation (Dallas et al., 2005). This was confirmed in the present study using fluorescent probes for these ECM proteins. We have also shown, using a fibronectin-null cell culture system, that fibronectin is required for assembly of LTBP1 but that fibronectin appears to be more rapidly turned over than LTBP1 (Dallas et al., 2005). Based on these observations, our working hypothesis to account for the partitioning of LTBP1 and fibronectin in mature FRC cultures is that fibronectin may form a temporary template for the initial deposition of LTBP1, which is later lost, leaving the LTBP1 fibrils in place. Another possibility is that there is either a cell-mediated reorganization of the original ECM components into new structures or that there is a breakdown of the original ECM, followed by assembly of a more highly organized ECM. Future studies are therefore required to address this and to determine the potential role of cell-mediated matrix reorganization in this ECM partitioning process.

To our knowledge, dynamic imaging of LTBP1 and fibronectin in mature FRC cultures has demonstrated for the first time that different ECM fibrillar networks within the same culture can show different dynamic properties. These differences in dynamic properties may be due to differences in the material properties of these fibrillar networks, their degree of crosslinking and/or differences in the proximity of the different networks to the cells. Our future goal is to determine how the dynamic properties of bone ECM proteins change during the process of matrix mineralization and in response to bone anabolic and catabolic agents.

In the present studies computational methods were used to quantify and correlate the dynamics of cell and ECM fibril motion in living osteoblasts. These analyses revealed that individual fibrils can stretch to as much as three and a half times their original length or contract up to one fourth of their original length. Rarely, individual fibrils were seen to break, with the two ends of the fibril showing elastic recoil. Together, these data suggest that the ECM fibrils exist in a state of tension and that osteoblasts can exert forces large enough to generate significant strains on individual fibrils. Current models of fibronectin assembly propose that mechanical stretching of cell surface integrin-bound fibronectin molecules is an essential step in the assembly process, which opens up the folded structure of the molecule, revealing cryptic 'self-association' sites (Pankov et al., 2000). These self-association sites then allow binding to other fibronectin molecules, enabling fibril polymerization. It therefore seems possible that cell-mediated stretching of fibronectin fibrils, as observed in our dynamic imaging studies, may contribute to the assembly process by

exposing additional cryptic binding sites in fibronectin molecules.

Vector correlation analysis, which statistically compares the direction of movement of cells and fibrils, suggested that their motion is correlated. We have also performed a more extensive 'local average correlation' in which vectors between the two images are compared within circles of increasing radius (data not shown). Interestingly, the extent of correlation of cell and fibril movement fell off as the radius increased, suggesting that the motion of ECM fibrils is primarily influenced by osteoblasts near to the fibrils, rather than by cells that are more distant. This is in contrast to studies using avian embryos, where the motion of fibrillin-2 fibrils was correlated to global tissue movements/deformations, and the distance over which cell and fibril movement was correlated increased with time in culture (Czirok et al., 2004).

In conclusion, our studies suggest that the assembly and reorganization of ECM proteins in living osteoblast cultures is a highly dynamic process that may be driven by cell motility. The dynamic properties of ECM proteins appear to change with ECM maturation and are different between different fibrillar networks within the same culture. Cell-mediated shunting and exchange of ECM material may represent a previously unknown mechanism for initial ECM assembly and reorganization that may have important implications for our understanding of the process of ECM assembly in living organisms.

Materials and Methods

Cell culture

Cell culture reagents were purchased from Cellgro, Mediatech Inc. (Herndon, VA). Primary FRCs were isolated as described previously (Dallas et al., 1995) and maintained in α-MEM supplemented with 10% Fetal Bovine Serum (FBS), 2 mM L-glutamine (LG), 100 U/ml penicillin/streptomycin (P/S) and 300 μg/ml gentamycin.

Fluorescently labeled fibronectin and LTBP1 probes

The probe for dynamic imaging of fibronectin was prepared by labeling 1 mg human plasma fibronectin (Life Technologies) using an Alexa Fluor 488 (green, emission 519 nm) or Alexa Fluor 555 (red, emission 565 nm) protein labeling kit, according to the manufacturer's instructions (Molecular Probes, Eugene, OR). For dynamic imaging of LTBP1, an affinity-purified rabbit polyclonal antibody to LTBP1 was used. This antibody has been described previously (Dallas et al., 2000). 1 mg anti-LTBP1 antibody was labeled with a Cy3 protein labeling kit (red, emission 565 nm) according to the manufacturer's instructions (Amersham Biosciences, Piscataway, NJ).

To determine the optimal times for probe incubation, FRC cells were plated in eight-well Lab-Tek chamber slides at 20,000 cells per well in 0.5 ml α-MEM supplemented with 10% FBS, 2 mM LG, 100 U/ml P/S and 300 μg/ml gentamycin. Three day postconfluent cultures were incubated for 24 hours with 5 μg/ml Alexa Fluor 488-labeled human plasma fibronectin and Cy3-labeled anti-LTBP1 antibody. The cells were then imaged after 1.5, 4, 6, 8 and 24 hours of incubation. After 24 hours, the probes were removed and the cells were washed four times with PBS. Stability of the incorporated probes was then monitored by taking images at time points between 1 and 10 days after removal of the probes. A Nikon TE300 Inverted Microscope was used under epifluorescent illumination. Digital images were obtained at 20× magnification with an Optronics CCD camera (Optronics, Goleta, CA).

Dynamic time-lapse imaging of fluorescently labeled fibronectin and LTBP1 fibrils in living osteoblast cultures

A Bioptechs Stage Incubator (Bioptechs, Butler, PA) was used for maintaining osteoblasts for live-cell microscopy. FRC cells were plated on Bioptechs culture dishes at 80,000 cells/dish and grown in culture for different time periods from 1-12 days. Based on results from the optimization experiments above, the FRC cells were incubated for 3 hours with 5 μg/ml of Alexa Fluor 488-labeled fibronectin or Cy3-labeled anti-LTBP1 antibody, or a combination of both probes. The media containing the fluorescent probes was then aspirated and the cells were washed five times in PBS, then fed with fresh media. The Bioptechs dishes were connected to a Bioptechs temperature controller, which directly heats the indium tin-oxide coated glass culture substrate. The temperature was maintained at 37°C and CO_2 was perfused through a calibrated peristaltic pump, to maintain the CO_2 concentration at 5%.

The cultures were imaged using a Leica DM-IRE2 inverted microscope (Leica) equipped with a Ludl Scientific Products automated shutter and motorized *X*, *Y* and *Z* stage controller together with a Q-Imaging cooled CCD camera with 12-bit grey scale resolution. A 20× objective was used and exposure times were approximately 100 mseconds for differential interference contrast (DIC) and 250 mseconds for fluorescence. Fields of 428×340 μm were imaged at a spatial resolution of 634×512 pixels (2×2 binned mode). Images from four to five independent fields and three to five focal planes were acquired in DIC and fluorescence modes using a computer-driven automated image acquisition system as described previously (Czirok et al., 2002). Image processing software (Czirok et al., 2002) selected the best focused optical plane from the acquired *Z* stacks, and the images were assembled into movies using Quicktime Pro.

Computational analyses of fibril and cell dynamics

Sequential time-lapse images were used to obtain quantitative length measurements on fibrils that showed stretching and/or contraction. Two fiducial marks were identified on each individual fibril to be measured, which included fibril ends, branch points or protuberances (bulges) on the fibril surface. The fibril distance between these two markers was measured from image stacks using the AnalySIS Image Processing Software (Soft Imaging System Corp, Lakewood, CO). A minimum of fifteen fibrils, taken from five independently imaged fields, were measured for each experimental group. The maximum and minimum percent stretch and percent contraction were determined from measurements for each fibril.

To analyze the overall cell and fibril displacements observed in the movies, a custom written program called 'X-TRACK' was used (Czirok et al., 2004). This software, operated on a Linux system, allows us to scroll through sequential images in an image stack. A set of 100 point markers were manually positioned on recognizable features in a still image of cells or fibrils from a time-lapse series. The same features were identified on an image obtained 1 hour later, and the markers repositioned. The net displacement of each point marker was then calculated using the two-point distance formula. The types of image feature markers selected included protrusions on fibrils, kinks on a fibril, or places where two or more fibrils join. Given that the co-ordinates of the points on the two images (separated by an hour) are (X_1,Y_1) and (X_2,Y_2) respectively, then the displacement is given by the two point distance formula: Magnitude of Displacement=$\sqrt{[(X_2–X_1)^2+(Y_2–Y_1)^2]}$. Frequency plots of the displacements were made and the mean displacements of point markers on cell or fibril images were calculated.

Correlation of cell and fibril movement

A custom program called 'VECTORPLOT' was written using the C# program to generate vector maps depicting the direction of movement of point markers between image frames separated by 1 hour. Given the initial and final co-ordinates of a point marker, the software plots a vector depicting the magnitude and direction of movement of the point marker. This software was validated by creating a set of synthetic vectors with known co-ordinates. The resulting vector map was then compared to the ground truth (known direction of movement of the vector).

To compare the direction of movement of vectors between cell and fibril images, we developed a software called 'local average correlation' (written using C^{++}). This program compares the direction of movement of vectors averaged within equivalent local neighborhoods between the two comparison images. By comparing average vectors rather than individual pairs of nearest-neighbor vectors, a more accurate comparison is obtained, because this approach reduces error from individual vectors that do not follow the local pattern of motion.

The software uses the origin of each vector on the first vector map as an anchor point and selects all vectors within a 30 μm radius (average radius of a cell in the field) around the point. The average of all these vectors is then determined as follows: (i) Let us assume that there are three fibril vectors, V_2, V_3 and V_4 within a 30 μm radius surrounding the anchor vector, V_1; (ii) The projection of each fibril vector on the *X* and *Y* axes were obtained as: projection on *X* axis=$R_x=V_{1x}+V_{2x}+V_{3x}+V_{4x}$; Projection on *Y* axis=$R_y=V_{1y}+V_{2y}+V_{3y}+V_{4y}$. The average of the fibril vectors (R) is given by $R=\sqrt{(R_x^2+R_y^2)}$. Given that the initial and final co-ordinates of the resultant vector are (X_1,Y_1) and (X_2,Y_2) respectively, then the angle of this average vector (θ1) from a horizontal reference line is given by: $\theta1=\tan^{-1}[(Y_2–Y_1)/(X_2–X_1)]$.

Vectors in an identical circle are then selected on the second (comparison) image, the average vector is calculated and its angle (θ2) from a horizontal reference line is determined as above. The pairs of angles of average vectors from equivalent neighborhoods in each image are then plotted, and the correlation coefficient calculated. A number of exclusion criteria were written into the program, as described: (1) Point markers that do not show any movement do not have a vector component associated with them, and were therefore excluded from the analysis. (2) θ1–θ2 values can range only from 0° (two vectors moving in same direction) to 180° (two vectors moving in the opposite direction). Therefore, the smallest possible angle between the vectors was used, as indicated below: If θ1>θ2 and θ1–θ2>π, then adjusted θ1=θ1–2π. If θ2>θ1 and θ2–θ1>π, then adjusted θ2=θ2–2π.

The 'local average correlation' software was validated by creating two sets of synthetic vectors with known co-ordinates, and comparing their correlation coefficient with the ground truth. The circle of 30 μm radius was chosen because it represents the approximate diameter of a cell in the field, and is based on the assumption that the movement of fibrils will be more closely related to cells that are in the vicinity of the fibrils rather than cells that are further away. The assumption was supported by performing a similar analysis using circles of increasing radius, showing that the angle difference between pairs of vectors became more random with increasing distance from the anchor vector (data not shown).

We are very grateful to Charles Little for envisioning and implementing hardware and software to perform time-lapse imaging at the University of Kansas Medical Center. Use of these shared resources is greatly appreciated. We thank Karen Williams (University of Missouri, Kansas City) for her valuable help in statistical analyses. We also thank Lynda Bonewald for critical review of the manuscript. This work was supported by NIH grant AR051517 to S.L.D. and in part by Kansas City Area Life Sciences grant KCALSI-04-03 to P.S., Hungarian Research Fund OTKA T047055 to A.C., and NIH grants HL73700 to B.J.R. and CA75387 to S.L.D.

References

Annes, J. P., Chen, Y., Munger, J. S. and Rifkin, D. B. (2004). Integrin {alpha}V{beta}6-mediated activation of latent TGF-{beta} requires the latent TGF-{beta} binding protein-1. *J. Cell Biol.* **165**, 723-734.

Corson, G. M., Charbonneau, N. L., Keene, D. R. and Sakai, L. Y. (2004). Differential expression of fibrillin-3 adds to microfibril variety in human and avian, but not rodent, connective tissues. *Genomics* **83**, 461-472.

Czirok, A., Rupp, P. A., Rongish, B. J. and Little, C. D. (2002). Multi-field 3D scanning light microscopy of early embryogenesis. *J. Microsc.* **206**, 209-217.

Czirok, A., Rongish, B. J. and Little, C. D. (2004). Extracellular matrix dynamics during vertebrate axis formation. *Dev. Biol.* **268**, 111-122.

Czirok, A., Zach, J., Kozel, B. A., Mecham, R. P., Davis, E. C. and Rongish, B. J. (2006). Elastic fiber macro-assembly is a hierarchical cell motion-mediated process. *J. Cell. Physiol.* **207**, 97-106.

Dallas, S. L., Miyazono, K., Skerry, T. M., Mundy, G. R. and Bonewald, L. F. (1995). Dual role for the latent transforming growth factor-beta binding protein in storage of latent TGF-beta in the extracellular matrix and as a structural matrix protein. *J. Cell Biol.* **131**, 539-549.

Dallas, S. L., Keene, D. R., Bruder, S. P., Saharinen, J., Sakai, L. Y., Mundy, G. R. and Bonewald, L. F. (2000). Role of the latent transforming growth factor beta binding protein 1 in fibrillin-containing microfibrils in bone cells in vitro and in vivo. *J. Bone Miner. Res.* **15**, 68-81.

Dallas, S. L., Rosser, J. L., Mundy, G. R. and Bonewald, L. F. (2002). Proteolysis of latent-TGFbeta binding protein-1 by osteoclasts – a cellular mechanism for release of TGFbeta from bone matrix. *J. Biol. Chem.* **277**, 21352-21360.

Dallas, S. L., Sivakumar, P., Jones, C. J., Chen, Q., Peters, D. M., Mosher, D. F., Humphries, M. J. and Kielty, C. M. (2005). Fibronectin regulates latent transforming growth factor-{beta} (TGF{beta}) by controlling matrix assembly of latent TGF{beta}-binding protein-1. *J. Biol. Chem* **280**, 18871-18880.

Davidson, L. A., Keller, R. and DeSimone, D. W. (2004). Assembly and remodeling of the fibrillar fibronectin extracellular matrix during gastrulation and neurulation in Xenopus laevis. *Dev. Dyn.* **231**, 888-895.

Day, R. N. and Schaufele, F. (2005). Imaging molecular interactions in living cells. *Mol. Endocrinol.* **19**, 1675-1686.

Eils, R. and Athale, C. (2003). Computational imaging in cell biology. *J. Cell Biol.* **161**, 477-481.

Filla, M. B., Czirok, A., Zamir, E. A., Little, C. D., Cheuvront, T. J. and Rongish, B. J. (2004). Dynamic imaging of cell, extracellular matrix, and tissue movements during avian vertebral axis patterning. *Birth Defects Res. C Embryo Today* **72**, 267-276.

Flaumenhaft, R., Abe, M., Sato, Y., Miyazono, K., Harpel, J., Heldin, C. H. and Rifkin, D. B. (1993). Role of the latent TGF-beta binding protein in the activation of latent TGF-beta by co-cultures of endothelial and smooth muscle cells. *J. Cell Biol.* **120**, 995-1002.

Globus, R. K., Doty, S. B., Lull, J. C., Holmuhamedov, E., Humphries, M. J. and Damsky, C. H. (1998). Fibronectin is a survival factor for differentiated osteoblasts. *J. Cell Sci.* **111**, 1385-1393.

Godyna, S., Mann, D. M. and Argraves, W. S. (1995). A quantitative analysis of the incorporation of fibulin-1 into extracellular matrix indicates that fibronectin assembly is required. *Matrix Biol.* **14**, 467-477.

Gronowicz, G. A., DeRome, M. E. and McCarthy, M. B. (1991). Glucocorticoids inhibit fibronectin synthesis and messenger ribonucleic acid levels in cultured fetal rat parietal bones. *Endocrinology* **128**, 1107-1114.

Guise, T. A. and Chirgwin, J. M. (2003). Transforming growth factor-beta in osteolytic breast cancer bone metastases. *Clin. Orthop. Relat. Res.* **415**, S32-S38.

Hyytiainen, M., Penttinen, C. and Keski-Oja, J. (2004). Latent TGF-beta binding proteins: extracellular matrix association and roles in TGF-beta activation. *Crit. Rev. Clin. Lab. Sci.* **41**, 233-264.

Janssens, K., Gershoni-Baruch, R., Guanabens, N., Migone, N., Ralston, S., Bonduelle, M., Lissens, W., Van Maldergem, L., Vanhoenacker, F., Verbruggen, L. et al. (2000). Mutations in the gene encoding the latency-associated peptide of TGF-beta 1 cause Camurati-Engelmann disease. *Nat. Genet.* **26**, 273-275.

Jones, E. A., Baron, M. H., Fraser, S. E. and Dickinson, M. E. (2005). Dynamic in vivo imaging of mammalian hematovascular development using whole embryo culture. *Methods Mol. Med.* **105**, 381-394.

Kielty, C. M., Wess, T. J., Haston, L., Ashworth, J. L., Sherratt, M. J. and Shuttleworth, C. A. (2002). Fibrillin-rich microfibrils: elastic biopolymers of the extracellular matrix. *J. Muscle Res. Cell Motil.* **23**, 581-596.

Kinoshita, A., Saito, T., Tomita, H., Makita, Y., Yoshida, K., Ghadami, M., Yamada, K., Kondo, S., Ikegawa, S., Nishimura, G. et al. (2000). Domain-specific mutations in TGFB1 result in Camurati-Engelmann disease. *Nat. Genet.* **26**, 19-20.

Kozel, B. A., Rongish, B. J., Czirok, A., Zach, J., Little, C. D., Davis, E. C., Knutsen, R. H., Wagenseil, J. E., Levy, M. A. and Mecham, R. P. (2006). Elastic fiber formation: A dynamic view of extracellular matrix assembly using times reporters. *J. Cell. Physiol.* **207**, 87-96.

Langdahl, B. L., Carstens, M., Stenkjaer, L. and Eriksen, E. F. (2003). Polymorphisms in the transforming growth factor beta 1 gene and osteoporosis. *Bone* **32**, 297-310.

McDonald, J. A., Kelley, D. G. and Broekelmann, T. J. (1982). Role of fibronectin in collagen deposition: Fab′ to the gelatin-binding domain of fibronectin inhibits both fibronectin and collagen organization in fibroblast extracellular matrix. *J. Cell Biol.* **92**, 485-492.

Miyazono, K., Olofsson, A., Colosetti, P. and Heldin, C. H. (1991). A role of the latent TGF-beta 1-binding protein in the assembly and secretion of TGF-beta 1. *EMBO J.* **10**, 1091-1101.

Moursi, A. M., Damsky, C. H., Lull, J., Zimmerman, D., Doty, S. B., Aota, S. and Globus, R. K. (1996). Fibronectin regulates calvarial osteoblast differentiation. *J. Cell Sci.* **109**, 1369-1380.

Nordahl, J., Mengarelli-Widholm, S., Hultenby, K. and Reinholt, F. P. (1995). Ultrastructural immunolocalization of fibronectin in epiphyseal and metaphyseal bone of young rats. *Calcif. Tissue Int.* **57**, 442-449.

Ohashi, T., Kiehart, D. P. and Erickson, H. P. (1999). Dynamics and elasticity of the fibronectin matrix in living cell culture visualized by fibronectin-green fluorescent protein. *Proc. Natl. Acad. Sci. USA* **96**, 2153-2158.

Ohashi, T., Kiehart, D. P. and Erickson, H. P. (2002). Dual labeling of the fibronectin matrix and actin cytoskeleton with green fluorescent protein variants. *J. Cell Sci.* **115**, 1221-1229.

Pankov, R., Cukierman, E., Katz, B. Z., Matsumoto, K., Lin, D. C., Lin, S., Hahn, C. and Yamada, K. M. (2000). Integrin dynamics and matrix assembly: tensin-dependent translocation of alpha(5)beta(1) integrins promotes early fibronectin fibrillogenesis. *J. Cell Biol.* **148**, 1075-1090.

Parsons, M., Vojnovic, B. and Ameer-Beg, S. (2004). Imaging protein-protein interactions in cell motility using fluorescence resonance energy transfer (FRET). *Biochem. Soc. Trans.* **32**, 431-433.

Pereira, M., Rybarczyk, B. J., Odrljin, T. M., Hocking, D. C., Sottile, J. and Simpson-Haidaris, P. J. (2002). The incorporation of fibrinogen into extracellular matrix is dependent on active assembly of a fibronectin matrix. *J. Cell Sci.* **115**, 609-617.

Petroll, W. M. and Ma, L. (2003). Direct, dynamic assessment of cell-matrix interactions inside fibrillar collagen lattices. *Cell Motil. Cytoskeleton* **55**, 254-264.

Petroll, W. M., Ma, L. and Jester, J. V. (2003). Direct correlation of collagen matrix deformation with focal adhesion dynamics in living corneal fibroblasts. *J. Cell Sci.* **116**, 1481-1491.

Petroll, W. M., Cavanagh, H. D. and Jester, J. V. (2004). Dynamic three-dimensional visualization of collagen matrix remodeling and cytoskeletal organization in living corneal fibroblasts. *Scanning* **26**, 1-10.

Pujol, J. P. (1999). TGF-beta and osteoarthritis: in vivo veritas? *Osteoarthritis Cartilage* **7**, 439-440.

Ramirez, F. and Pereira, L. (1999). The fibrillins. *Int. J. Biochem. Cell Biol.* **31**, 255-259.

Roman, J. and McDonald, J. A. (1993). Fibulin's organization into the extracellular matrix of fetal lung fibroblasts is dependent on fibronectin matrix assembly. *Am. J. Respir. Cell Mol. Biol.* **8**, 538-545.

Sakai, T. (2003). Video-imaging visualization of blood flow dynamics in early chick embryo. *Jpn. J. Physiol.* **53**, 385-388.

Sekar, R. B. and Periasamy, A. (2003). Fluorescence resonance energy transfer (FRET) microscopy imaging of live cell protein localizations. *J. Cell Biol.* **160**, 629-633.

Sottile, J. and Hocking, D. C. (2002). Fibronectin polymerization regulates the composition and stability of extracellular matrix fibrils and cell-matrix adhesions. *Mol. Biol. Cell* **13**, 3546-3559.

Taipale, J., Miyazono, K., Heldin, C. H. and Keski-Oja, J. (1994). Latent transforming growth factor-beta 1 associates to fibroblast extracellular matrix via latent TGF-beta binding protein. *J. Cell Biol.* **124**, 171-181.

Taipale, J., Saharinen, J., Hedman, K. and Keski-Oja, J. (1996). Latent transforming growth factor-beta 1 and its binding protein are components of extracellular matrix microfibrils. *J. Histochem. Cytochem.* **44**, 875-889.

Velling, T., Risteli, J., Wennerberg, K., Mosher, D. F. and Johansson, S. (2002). Polymerization of type I and III collagens is dependent on fibronectin and enhanced by integrins alpha 11beta 1 and alpha 2beta 1. *J. Biol. Chem* **277**, 37377-37381.

Young, M. F. (2003). Bone matrix proteins: their function, regulation, and relationship to osteoporosis. *Osteoporos. Int.* **14**, S35-S42.